molecules

MDPI

Supplementary Materials

Article

QM/MM Benchmarking of Cyanobacteriochrome Slr1393g3 Absorption Spectra

Christian Wiebeler † and Igor Schapiro *

Fritz Haber Center for Molecular Dynamics Research, Institute of Chemistry, The Hebrew University of Jerusalem, Jerusalem 91904, Israel; chwie@mail.upb.de

* Correspondence: Igor.Schapiro@mail.huji.ac.il

† Current address: Physics Department, Universität Paderborn, 33098 Paderborn, Germany

Table 1. Root mean square deviations of geometries in Å. Comparisons are given for methods in the corresponding column and row for P_r (first value) and P_g (second value, shown in parenthesis).

P_r (P_g)	PM3	PM3-PDDG	RI-CC2
MNDO	0.54 (0.67)	0.53 (0.59)	0.98 (1.27)
PM3	-	0.28 (0.54)	0.99 (1.26)
PM3-PDDG		-	1.15 (1.60)

Table S2. Root mean square deviations of geometries in Å. Comparisons are given for methods in the corresponding column and row for P_r (first value) and P_g (second value, shown in parenthesis).

P_r (P_g)	PM6-D	PM6-DH+	RI-CC2
PM6	0.06 (0.15)	0.11 (0.27)	0.87 (1.34)
PM6-D	-	0.06 (0.14)	0.82 (1.22)
PM6-DH+		-	0.76 (1.10)

Table S3. Root mean square deviations of geometries in Å. Comparisons are given for methods in the corresponding column and row for P_r (first value) and P_g (second value, shown in parenthesis).

P_r (P_g)	AM1/d	AM1-D	AM1-DH+	RM1	RI-CC2
AM1	0.27 (0.37)	0.19 (0.27)	0.24 (0.28)	0.35 (0.40)	0.85 (1.17)
AM1/d	-	0.16 (0.25)	0.18 (0.24)	0.37 (0.12)	0.73 (1.10)
AM1-D		-	0.13 (0.13)	0.31 (0.21)	0.68 (0.96)
AM1-DH+			-	0.32 (0.23)	0.67 (0.96)
RM1				-	0.65 (1.02)

Table S4. Root mean square deviations of geometries in Å. Comparisons are given for methods in the corresponding column and row for P_r (first value) and P_g (second value, shown in parenthesis).

P_r (P_g)	DFTB3	DFTB2+D	RI-CC2
DFTB2	0.12 (0.13)	0.22 (0.80)	0.79 (0.94)
DFTB3	-	0.33 (0.92)	0.89 (1.06)
DFTB2+D		-	0.58 (0.23)

Table S5. Excitation energies (E, in eV) and oscillator strengths (f) for the first 10 excited singlet states for P_r from RI-CC2/cc-pVDZ calculations based on structures optimized *in vacuo* with the method given as headline of the two columns.

P_r	RI-CC2		DFTB2+D		DFTB2		DFTB3		AM1-DH+		PM6-DH+		RM1	
	E	f	E	f	E	f	E	f	E	f	E	f	E	f
S_1	2.01	0.825	2.16	1.154	2.18	1.261	2.20	1.319	2.23	1.118	2.24	1.199	2.25	1.131
S_2	3.19	0.228	3.35	0.237	3.39	0.230	3.40	0.000	3.37	0.271	3.35	0.300	3.33	0.299
S_3	3.35	0.000	3.42	0.000	3.43	0.000	3.40	0.237	3.48	0.000	3.73	0.000	3.57	0.001
S_4	3.78	0.410	3.85	0.363	3.85	0.361	3.88	0.352	3.99	0.213	3.92	0.121	3.98	0.054
S_5	4.04	0.152	4.11	0.103	4.14	0.109	4.16	0.114	4.06	0.090	3.99	0.124	3.99	0.170
S_6	4.08	0.006	4.28	0.045	4.30	0.038	4.30	0.037	4.24	0.089	4.24	0.097	4.23	0.095
S_7	4.21	0.051	4.34	0.060	4.35	0.038	4.37	0.067	4.34	0.059	4.36	0.051	4.39	0.037
S_8	4.40	0.295	4.56	0.156	4.38	0.034	4.43	0.008	4.49	0.000	4.70	0.243	4.58	0.003
S_9	4.48	0.003	4.63	0.022	4.63	0.049	4.55	0.001	4.64	0.233	4.71	0.015	4.70	0.209
S_{10}	4.71	0.150	4.65	0.110	4.63	0.222	4.65	0.266	4.91	0.097	4.94	0.090	4.99	0.126

Table S6. Excitation energies (E, in eV) and oscillator strengths (f) for the first 10 excited singlet states for P_g from RI-CC2/cc-pVDZ calculations based on structures optimized *in vacuo* with the method given as headline of the two columns.

P_g	RI-CC2		DFTB2+D		DFTB2		DFTB3		AM1-DH+		PM6-DH+		RM1	
	E	f	E	f	E	f	E	f	E	f	E	f	E	f
S_1	2.00	0.747	2.06	0.828	2.17	1.211	2.19	1.271	2.24	1.061	2.28	1.125	2.29	0.994
S_2	3.20	0.252	3.27	0.262	3.38	0.000	3.35	0.000	3.37	0.355	3.35	0.386	3.31	0.352
S_3	3.24	0.001	3.31	0.001	3.41	0.219	3.43	0.250	3.44	0.011	3.71	0.000	3.58	0.001
S_4	3.61	0.491	3.61	0.449	3.61	0.468	3.66	0.453	3.90	0.271	3.87	0.164	3.98	0.069
S_5	4.02	0.014	4.06	0.008	4.19	0.010	4.21	0.012	4.06	0.025	3.98	0.029	4.01	0.191
S_6	4.07	0.027	4.19	0.016	4.31	0.015	4.32	0.015	4.26	0.045	4.28	0.045	4.26	0.058
S_7	4.21	0.068	4.28	0.056	4.35	0.015	4.38	0.028	4.36	0.067	4.36	0.082	4.38	0.064
S_8	4.47	0.415	4.57	0.424	4.39	0.061	4.40	0.049	4.50	0.002	4.72	0.004	4.58	0.003
S_9	4.52	0.001	4.68	0.048	4.67	0.001	4.59	0.000	4.67	0.238	4.74	0.215	4.73	0.170
S_{10}	4.66	0.164	4.73	0.100	4.69	0.377	4.71	0.364	4.86	0.150	4.90	0.152	4.94	0.149

Table S7. Lowest energy absorption maxima of P_r and P_g from semiempirical methods. Wavelengths (λ), energies (E_{max}), energy differences in parenthesis and absolute absorption (ε_{Pr} and ε_{Pg}) as well as photoproduct tuning (ΔE_{max}) and ratio of absorption intensities ($\varepsilon_{Pg}/\varepsilon_{Pr}$) are tabulated. QM66 was employed and if not stated otherwise, the results are based on 10 snapshots taken every 100 ps and employing a cutoff of 12 Å to any of the QM atoms to take the environment as point charges into account.

Method	P_r			P_g			Comparison	
	λ (nm)	E_{max} (eV)	ε_{Pr}[3]	λ (nm)	E_{max} (eV)	ε_{Pg}[3]	ΔE_{max} (eV)	$\varepsilon_{Pg}/\varepsilon_{Pr}$
Exp.[1]	649	1.91	-	536	2.31	-	0.40	0.562
ZINDO/S								
100 geom.[2]	665	1.87 (-0.04)	8.17	606	2.05 (-0.27)	7.40	0.18	0.905
10 geom.[2]	657	1.89 (-0.02)	9.47	616	2.01 (-0.30)	8.47	0.13	0.893
24 Å cutoff	657	1.89 (-0.02)	9.11	621	2.00 (-0.32)	8.44	0.11	0.926
sTD-DFT								
100 geom.[2]	620	2.00 (+0.09)	7.80	550	2.26 (-0.06)	6.63	0.26	0.850
10 geom.[2]	614	2.02 (+0.11)	9.87	557	2.23 (-0.09)	8.97	0.21	0.909
24 Å cutoff	611	2.03 (+0.12)	9.29	561	2.21 (-0.10)	8.23	0.18	0.886
sTDA	572	2.17 (+0.26)	15.01	527	2.35 (+0.04)	12.90	0.18	0.859
sTD-DFT (ωB97)	530	2.34 (+0.43)	11.68	492	2.52 (+0.21)	9.93	0.18	0.850

[1] Taken from the spectra in Ref. [14] of the main text; [2] Values as reported in our previous publication, see Ref. [12] of the main text; [3] In units of 10^4 L/(mol cm).

Table S8. Lowest energy absorption maxima of P_r and P_g employing a QM region consisting of 106 atoms. Wavelengths (λ), energies (E_{max}), energy differences in parenthesis and absolute absorption (ε_{Pr} and ε_{Pg}) as well as photoproduct tuning (ΔE_{max}) and ratio of absorption intensities ($\varepsilon_{Pg}/\varepsilon_{Pr}$) are tabulated. The cc-pVDZ basis set in case of the RI-ADC(2) and B3LYP calculations was employed. If not stated otherwise, the results are based on 10 snapshots taken every 100 ps and employing a cutoff of 12 Å to any of the QM atoms to take the environment as point charges into account.

Method	P_r			P_g			Comparison	
	λ (nm)	**E_{max} (eV)**	**ε_{Pr}[3]**	**λ (nm)**	**E_{max} (eV)**	**ε_{Pg}[3]**	**ΔE_{max} (eV)**	**$\varepsilon_{Pg}/\varepsilon_{Pr}$**
Exp.[1]	649	1.91	-	536	2.31	-	0.40	0.562
RI-ADC(2)								
100 geom. [2]	628	1.97 (+0.06)	4.83	556	2.23 (-0.08)	3.90	0.26	0.808
10 geom. [2]	616	2.01 (+0.10)	8.44	568	2.18 (-0.13)	6.25	0.17	0.740
Full Virtual Space[2]	626	1.98 (+0.07)	8.46	577	2.15 (-0.16)	6.11	0.17	0.740
TD-DFT								
B3LYP	586	2.12 (+0.21)	8.88	567	2.19 (-0.13)	6.04	0.07	0.680
ZINDO/S								
100 geom. [2]	677	1.83 (-0.08)	7.63	608	2.04 (-0.27)	6.50	0.21	0.852
10 geom. [2]	673	1.84 (-0.07)	8.72	624	1.99 (-0.33)	6.85	0.14	0.785
24 Å cutoff	672	1.85 (-0.07)	8.69	622	1.99 (-0.32)	7.33	0.15	0.844
sTD-DFT								
100 geom. [2]	627	1.98 (+0.07)	7.02	553	2.24 (-0.07)	5.78	0.27	0.823
10 geom. [2]	621	2.00 (+0.09)	8.07	571	2.17 (-0.14)	6.80	0.18	0.843
24 Å cutoff	621	2.00 (+0.09)	8.41	563	2.20 (-0.11)	7.28	0.20	0.865
sTDA	580	2.14 (+0.23)	12.71	540	2.30 (-0.02)	9.95	0.16	0.783
sTD-DFT (ωB97)	544	2.28 (+0.37)	9.87	506	2.45 (+0.14)	8.66	0.17	0.878

[1] Taken from the spectra in Ref. [14] of the main text; [2] Values as reported in our previous publication, see Ref. [12] of the main text; [3] In units of 10^4 L/(mol cm).

Table S9. Lowest energy absorption maxima of P_r and P_g from multi-reference calculations. Wavelengths (λ), energies (E_{max}), energy differences in parenthesis and absolute absorption (ε_{Pr} and ε_{Pg}) as well as photoproduct tuning (ΔE_{max}) and ratio of absorption intensities ($\varepsilon_{Pg}/\varepsilon_{Pr}$) are tabulated. In all cases, the QM region consisted of 66 atoms and the results are based on 10 snapshots taken every 100 ps and employing a cutoff of 12 Å to any of the QM atoms to take the environment as point charges into account.

Method	P_r			P_g			Comparison	
	λ (nm)	**E_{max} (eV)**	**ε_{Pr}[2]**	**λ (nm)**	**E_{max} (eV)**	**ε_{Pg}[2]**	**ΔE_{max} (eV)**	**$\varepsilon_{Pg}/\varepsilon_{Pr}$**
Exp.[1]	649	1.91	-	536	2.31	-	0.40	0.562
NEVPT(2)								
PC (20/13)	588	2.11 (+0.20)	7.17	569	2.18 (-0.13)	7.75	0.07	1.082
SC (20/13)	556	2.23 (+0.32)	7.91	536	2.31 (+0.00)	8.39	0.08	1.060
OM2-MRCISD								
(40/40)	580	2.14 (+0.23)	9.33	537	2.31 (+0.00)	9.55	0.17	1.023
(20/20)	550	2.25 (+0.34)	10.58	510	2.43 (+0.12)	10.31	0.18	0.974
(20/20) + Triples	570	2.17 (+0.26)	9.49	526	2.36 (+0.04)	9.36	0.18	0.986

[1] Taken from the spectra in Ref. [14] of the main text; [2] In units of 10^4 L/(mol cm).

Table S10. Root mean square deviations of geometries in Å. Comparisons are given for methods in the corresponding column and row for P_r (first value) and P_g (second value, shown in parenthesis). For alignment, the geometries were reduced to 42 atoms as in case of the optimizations *in vacuo*. They were obtained from RI-BLYP+D3/AMBER optimized structures, where the QM region either consisted of 106 atoms (QM106) or 66 atoms (QM66). In case of the latter, optimizations were not only performed in cartesian coordinates, but also in hybrid delocalized coordinates (HDLC).

P_r (P_g)	QM66	QM66 HDLC
QM106	0.08 (0.08)	0.08 (0.07)
QM66	-	0.03 (0.03)

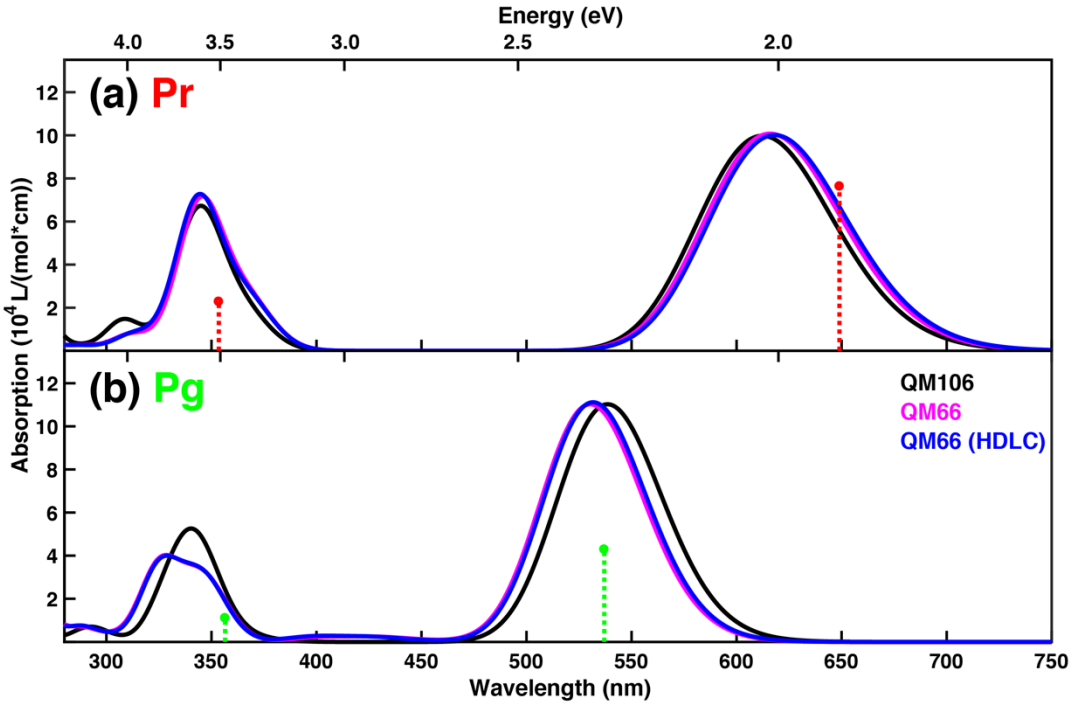

Figure S1. (**a**) Absorption spectra for RI-BLYP+D3/AMBER optimized structures with QM66 or QM106 (black) from subsequent sTD-DFT calculations for the P_r form employing QM106 for the excited state calculations. In case of the smaller QM region for optimization, either cartesian (magenta) or hybrid delocalized coordinates (HDLC, blue) were used; (**b**) Absorption spectra for RI-BLYP+D3/AMBER optimized structures from subsequent sTD-DFT calculations for the P_g form analogous to the results from P_r.

Table S11. Lowest energy absorption maxima of P_r and P_g from sTD-DFT calculations for RI-BLYP+D3/AMBER optimized structures. Wavelengths (λ), energies (E_{max}), energy differences in parenthesis and absolute absorption (ε_{Pr} and ε_{Pg}) as well as photoproduct tuning (ΔE_{max}) and ratio of absorption intensities ($\varepsilon_{Pg}/\varepsilon_{Pr}$) are tabulated.. In all cases, the QM region for excited state calculations consisted of 106 atoms and the values are extracted from the spectra in Figure S1.

Method	P_r			P_g			Comparison	
	λ (nm)	E_{max} (eV)	ε_{Pr}[2]	λ (nm)	E_{max} (eV)	ε_{Pg}[2]	ΔE_{max} (eV)	$\varepsilon_{Pg}/\varepsilon_{Pr}$
Exp.[1]	649	1.91	-	536	2.31	-	0.40	0.562
QM106	612	2.03 (+0.12)	9.98	539	2.30 (-0.01)	11.02	0.28	1.105
QM66	616	2.01 (+0.10)	10.07	531	2.34 (+0.02)	11.02	0.32	1.094
QM66 + HDLC	618	2.01 (+0.10)	10.01	532	2.33 (+0.02)	11.11	0.33	1.110

[1] Taken from the spectra in Ref. [14] of the main text; [2] In units of 10^4 L/(mol cm).

Table S12. Root mean square deviations of geometries in Å. Comparisons are given for methods in the corresponding column and row for P_r (first value) and P_g (second value, in parenthesis). For alignment, the geometries were reduced to 42 atoms as in the case of the optimizations *in vacuo*. They were obtained from DFTB2+D/AMBER optimized structures with QM66. The structures denoted as "Initial" were obtained from 100,000 steps of steepest descent (SD) optimizations. Taking the final structure as starting point, up to 100,000 steps of further optimizations were performed with the conjugate gradient (CG), SD and a limited-memory Broyden-Fletcher-Goldfarb-Shanno algorithm implemented in XMIN (AMBER software package). However, for CG and XMIN the optimizations ended before reaching the maximum number of iterations. In addition, the DFTB2+D/AMBER optimizations results for 100,000 steps of SD starting from the RI-BLYP+D3/AMBER optimized structure are also shown (from BLYP).

P_r (P_g)	CG	SD	XMIN	From BLYP
Initial	0.01 (0.01)	0.00 (0.00)	0.01 (0.02)	0.04 (0.05)
CG	-	0.00 (0.01)	0.01 (0.01)	0.05 (0.05)
SD		-	0.01 (0.02)	0.04 (0.05)
XMIN			-	0.05 (0.06)

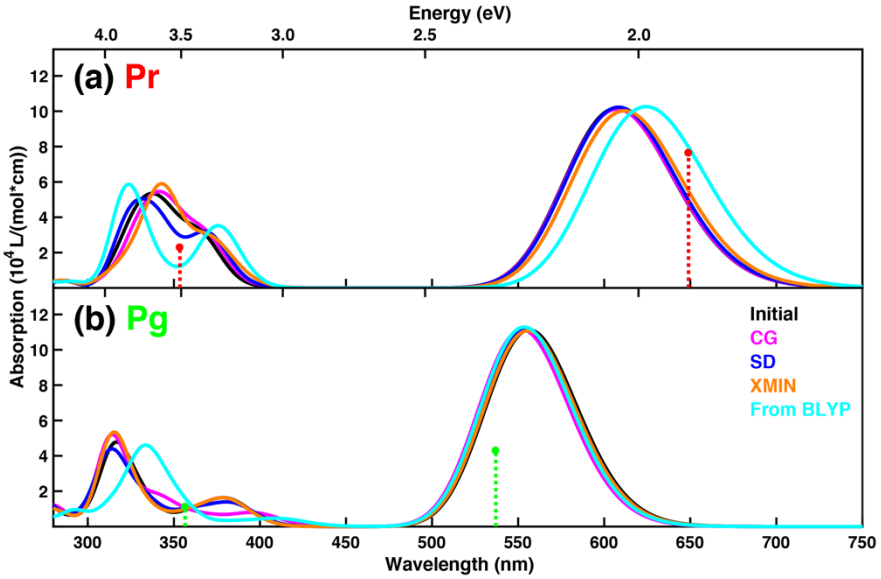

Figure S2. (**a**) Absorption spectra for DFTB2+D/AMBER optimized structures from subsequent sTD-DFT calculations for the P_r form employing 106 atoms. Shown are the spectra from structures of an initial 100,000 step steepest descent optimization (Initial, black), of subsequent optimizations employing up to 100,000 steps with conjugate gradient (CG, magenta), steepest descent (SD, blue), and a limited-memory Broyden-Fletcher-Goldfarb-Shanno algorithm implemented in XMIN (orange). In addition, the spectrum obtained from 100,000 steps of SD starting with the RI-BLYP+D3/AMBER optimized structure is also shown (From BLYP, cyan) and all optimizations were performed with QM66. (**b**) Absorption spectra for DFTB2+D/AMBER optimized structures from subsequent sTD-DFT calculations for the P_g form analogous to the results from P_r.

Table S13. Lowest energy absorption maxima of P_r and P_g from sTD-DFT calculations for DFTB2+D/AMBER optimized structures. Wavelengths (λ), energies (E_{max}), energy differences in parenthesis and absolute absorption (ε_{Pr} and ε_{Pg}) as well as photoproduct tuning (ΔE_{max}) and ratio of absorption intensities ($\varepsilon_{Pg}/\varepsilon_{Pr}$) are tabulated. In all cases, QM66 was employed for optimizations and QM106 for excited state calculations. The values are extracted from the spectra in Figure S2.

Method	**P_r**			**P_g**			**Comparison**	
	λ (nm)	**E_{max} (eV)**	**ε_{Pr}[2]**	**λ (nm)**	**E_{max} (eV)**	**ε_{Pg}[2]**	**ΔE_{max} (eV)**	**$\varepsilon_{Pg}/\varepsilon_{Pr}$**
Exp.[1]	649	1.91	-	536	2.31	-	0.40	0.562
Initial	607	2.04 (+0.13)	10.17	557	2.23 (-0.09)	11.13	0.19	1.094
CG	607	2.04 (+0.13)	10.12	552	2.25 (-0.07)	11.14	0.20	1.101
SD	608	2.04 (+0.13)	10.23	554	2.24 (-0.08)	11.18	0.20	1.093
XMIN	612	2.03 (+0.12)	10.02	556	2.23 (-0.08)	11.07	0.20	1.105
From BLYP	624	1.99 (+0.08)	10.26	553	2.24 (-0.07)	11.29	0.25	1.100

[1] Taken from the spectra in Ref. [14] of the main text; [2] In units of 10^4 L/(mol cm).

Table S14. Lowest energy absorption maxima of P_r and P_g from sTD-DFT calculations for (QM/)MM optimized structures. Wavelengths (λ), energies (E_{max}), energy differences in parenthesis and absolute absorption (ε_{Pr} and ε_{Pg}) as well as photoproduct tuning (ΔE_{max}) and ratio of absorption intensities ($\varepsilon_{Pg}/\varepsilon_{Pr}$) are tabulated. For QM/MM optimizations, QM66 was employed and QM106 was used in all cases for excited state calculations. The values are extracted from the spectra in Figure 3.

Method	P_r			P_g			Comparison	
	λ (nm)	E_{max} (eV)	ε_{Pr}[2]	λ (nm)	E_{max} (eV)	ε_{Pg}[2]	ΔE_{max} (eV)	$\varepsilon_{Pg}/\varepsilon_{Pr}$
Exp.[1]	649	1.91	-	536	2.31	-	0.40	0.562
RI-BLYP+D3	618	2.01 (+0.10)	10.01	532	2.33 (+0.02)	11.11	0.33	1.110
RI-MP2	600	2.07 (+0.16)	10.04	504	2.46 (+0.15)	10.92	0.40	1.088
RI-CC2	618	2.01 (+0.10)	9.73	511	2.43 (+0.11)	10.90	0.42	1.121
AMBER	703	1.76 (-0.15)	9.13	633	1.96 (-0.35)	9.97	0.19	1.092
DFTB2+D	607	2.04 (+0.13)	10.17	557	2.23 (-0.09)	11.13	0.19	1.094

[1] Taken from the spectra in Ref. [14] of the main text; [2] In units of 10^4 L/(mol cm).

Table S15. Arithmetic mean values of the excitation energies (E), oscillator strengths (f) and root mean square electron-hole separation (RMS_{eh}) for P_r and P_g as well as their differences obtained from wave function analysis for the lowest excited state with the exception of the BLYP calculations. In all cases, the QM region consisted of 66 atoms and if not stated otherwise, the results are based on 10 snapshots taken every 100 ps, the cc-pVDZ basis set was utilized, and a cutoff of 12 Å to any of the QM atoms was employed to take the environment as point charges into account.

Method	P_r			P_g			Difference		
	E (eV)	f	RMS_{eh}	E (eV)	f	RMS_{eh}	ΔE (eV)	Δf	ΔRMS_{eh}
RI-ADC(2)									
100 geom. [1]	2.040	1.049	5.108	2.272	1.040	4.813	0.231	-0.010	-0.295
10 geom.[1]	2.066	1.064	5.109	2.204	1.015	4.909	0.138	-0.049	-0.200
24 Å cutoff	2.075	1.075	5.049	2.205	1.027	4.869	0.131	-0.048	-0.180
cc-aug-pVDZ	2.014	1.016	5.233	2.144	0.955	4.998	0.130	-0.061	-0.235
WF-based									
RI-CC2	2.215	1.295	5.147	2.354	1.210	4.997	0.139	-0.085	-0.150
RI-CCS	2.757	1.557	4.681	2.932	1.529	4.357	0.175	-0.028	-0.324
CIS	2.758	1.581	4.277	2.933	1.541	3.996	0.175	-0.039	-0.282
TD-HF	2.506	1.409	4.221	2.681	1.389	3.938	0.175	-0.020	-0.283
DFT-based									
CAM-B3LYP	2.304	1.196	5.056	2.449	1.143	4.814	0.146	-0.053	-0.242
B3LYP	2.179	1.077	5.902	2.241	0.911	5.772	0.062	-0.166	-0.129
B3LYP (TDA)	2.468	1.681	6.160	2.459	1.272	5.990	-0.008	-0.410	-0.170
BLYP[2]	2.030	0.840	6.575	1.974	0.618	6.632	-0.056	-0.221	0.057

[1] Values from calculations reported in our previous study, see Ref. [12] of the main text; [2] For the statistics, we have considered excitations that are dominated by a transition from HOMO to LUMO. Owing to this and in case of BLYP, for 3 snapshots of P_r and 1 snapshot of P_g the S_2 state was considered, as in those cases the S_1 state was dominated by a charge transfer excitation from HOMO-1 to LUMO.

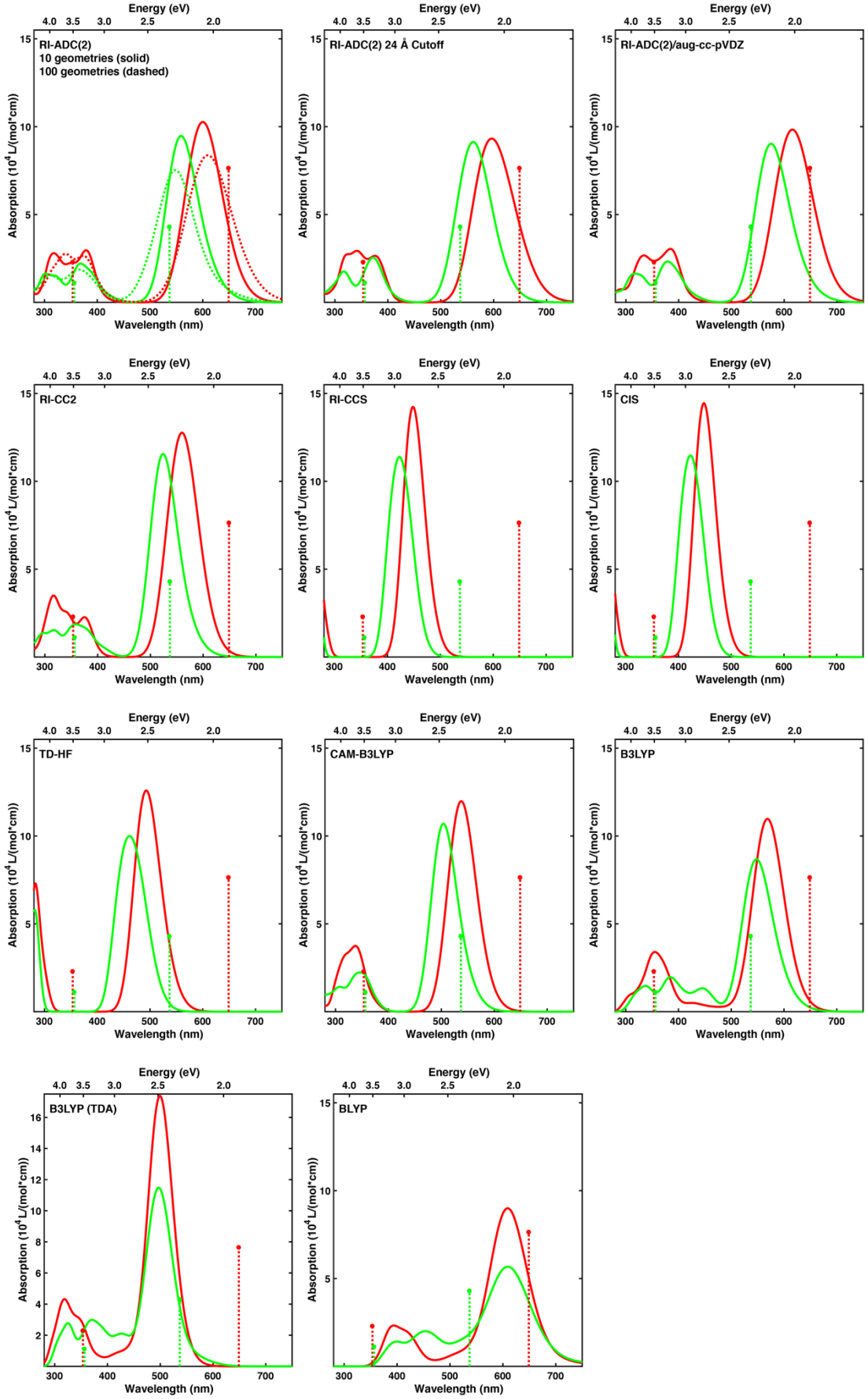

Figure S3: Spectra from which the values presented in Table 2 were derived and the corresponding method is indicated with an inset. For details of the computations, see the main text.

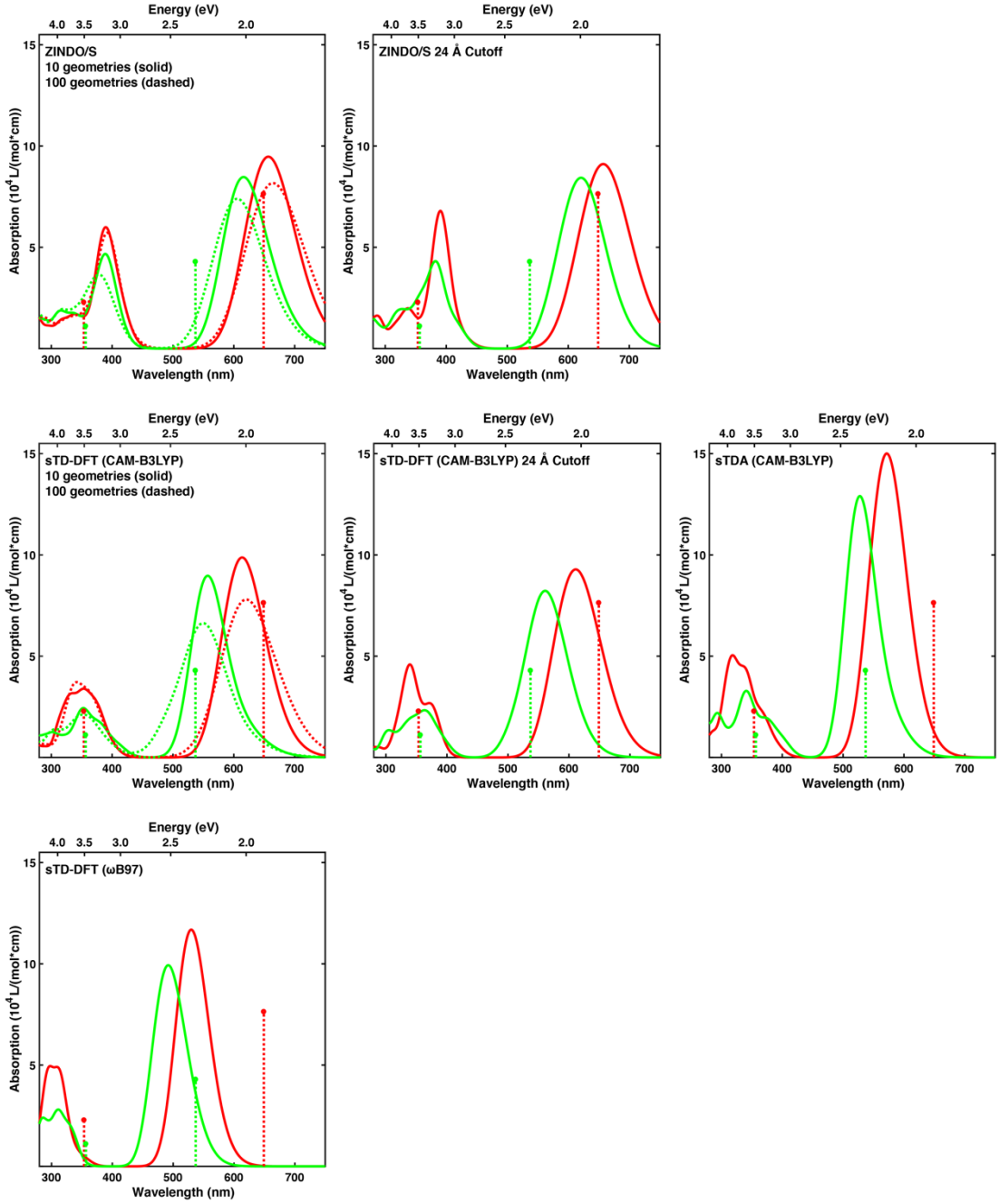

Figure S4: Spectra from which the values presented in Table S7 were derived and the corresponding method is indicated with an inset. For details of the computations, see the main text.

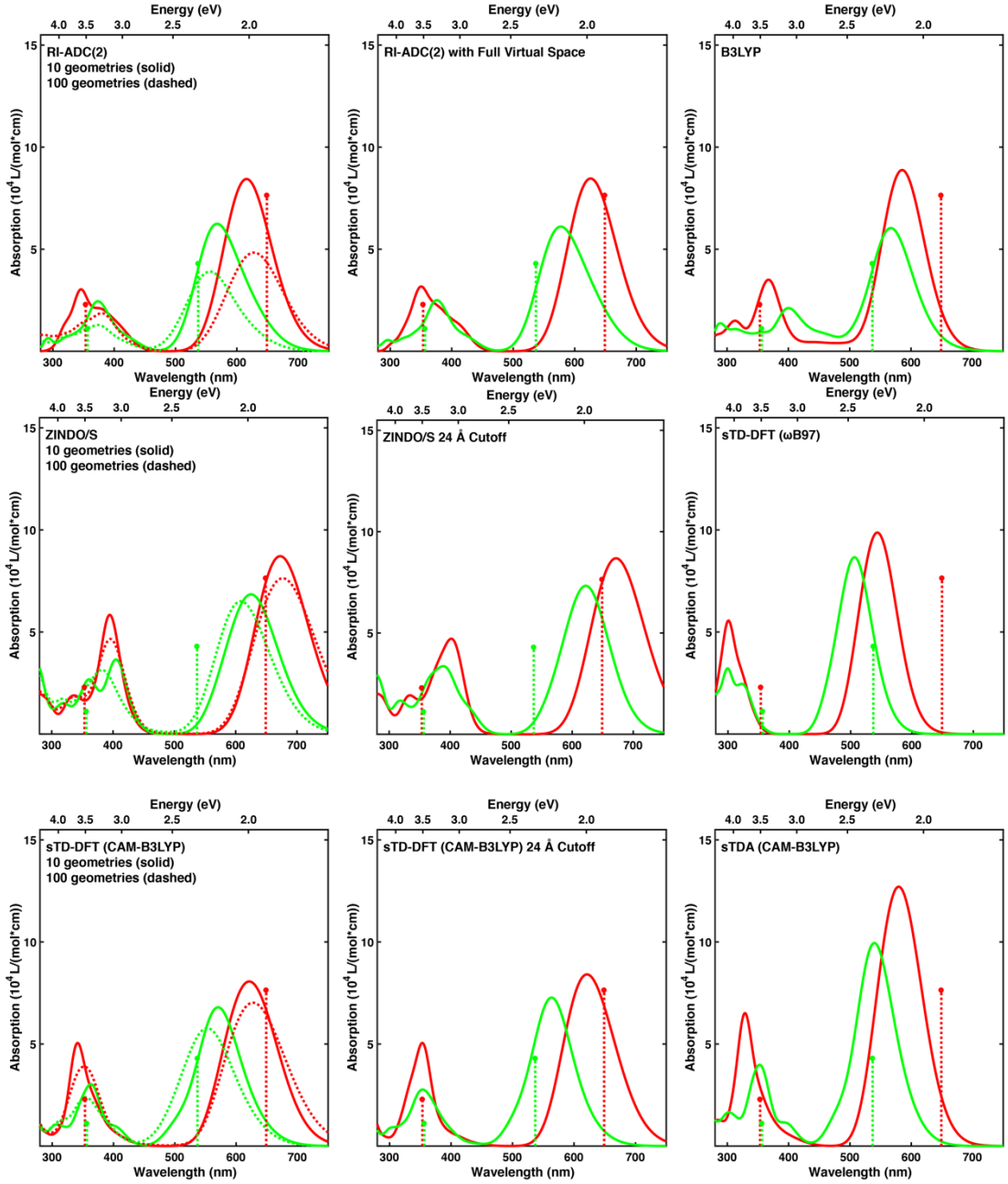

Figure S5: Spectra from which the values presented in Table S8 were derived, *i.e.* excited state calculations with QM106, and the corresponding method is indicated with an inset. For details of the computations, see the main text.

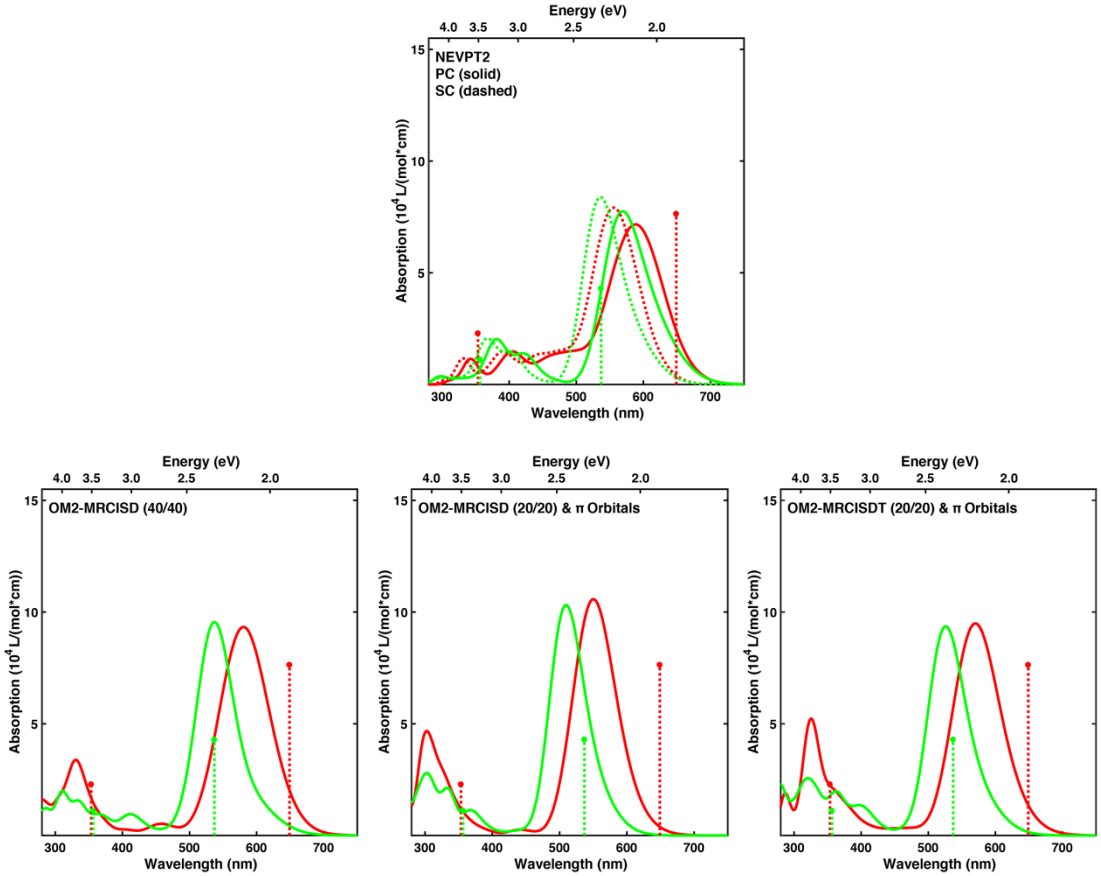

Figure S6: Spectra from which the values presented in Table S9 were derived and the corresponding method is indicated with an inset. For details of the computations, see the main text. Note that in case of the NEVPT2 calculations, the 5 excited states considered are not sufficient to cover the second absorption band.